Accepted Manuscript

On the properties of magnetorheological elastomers in shear mode: Design, fabrication and characterization

Ashkan Dargahi, Ramin Sedaghati, Subhash Rakheja

PII: S1359-8368(18)31147-8

DOI: 10.1016/j.compositesb.2018.09.080

Reference: JCOMB 6050

To appear in: *Composites Part B*

Received Date: 11 April 2018

Revised Date: 20 September 2018

Accepted Date: 24 September 2018

Please cite this article as: Dargahi A, Sedaghati R, Rakheja S, On the properties of magnetorheological elastomers in shear mode: Design, fabrication and characterization, *Composites Part B* (2018), doi: https://doi.org/10.1016/j.compositesb.2018.09.080.

On the Properties of Magnetorheological Elastomers in Shear Mode: Design, Fabrication and Characterization

Ashkan Dargahi [a], Ramin Sedaghati [b,*], Subhash Rakheja [c]

Department of Mechanical, Industrial and Aerospace Engineering, Concordia University, Montreal, QC H3G 1M8, Canada

[a] a_dargah@encs.concordia.ca, [b] ramin.sedaghati@concordia.ca, [c] subhash.rakheja@concordia.ca

Abstract

Magnetorheological elastomers (MREs) are novel class of magneto-active materials comprised of micron-sized ferromagnetic particles impregnated into an elastomeric matrix, which exhibit variable stiffness and damping properties in a reversible manner under the application of an external magnetic field. Characterization of highly complex behavior of these active composites is a fundamental necessity to design adaptive devices based on the MREs. This study is mainly concerned with in-depth experimental characterizations of static and dynamic properties of different types of MREs using methods defined in related standards. For this purpose, six different types of MRE samples with varying contents of rubber matrix and ferromagnetic particles were fabricated. The static characteristics of the samples were experimentally evaluated in shear mode as a function of the magnetic flux density. The particular MRE sample with highest iron particles content (40% volume fraction) was chosen for subsequent dynamic characterizations under broad ranges shear strain amplitude (2.5-20%), excitation frequency (0.1-50 Hz) and applied magnetic flux densities (0-450 mT). The results revealed nearly 1672% increase in the MRE storage modulus under the application of a magnetic flux of 450 mT, which confirms the potential of the novel fabricated MRE for control of vibration and noise in various engineering applications.

Keywords: Magnetorheological Elastomer; Fabrication; Characterization; Shear, Elastic and Loss Moduli

1. Introduction

Elastomers are rubber-like solids with viscoelastic properties, which are widely used as reliable and cost-effective passive damping treatments for attenuation of noise and vibration in many engineering applications. Such elastomers, owing to their fixed parameters, are known to be effective in a limited frequency range. Magnetorheological elastomers (MREs) are a class of smart composite materials, which exhibit reversible and rapid variations in their dynamic properties under the application of an external magnetic field. MREs are comprised of micron-sized ferromagnetic particles prearranged or suspended into an elastomeric matrix. Owing to their rapid response [1], the elastic moduli of these flexible smart composites can be effectively controlled in nearly real-time in response to varying external excitations. The MREs thus provide greater potential for suppression of vibration in an active manner in a wider range of frequencies [2, 3]. Moreover, MREs exhibit additional desirable features, such as low power requirement, fail-safe character, insensitivity to contaminants and no sealing issues (as generally

encountered in MR fluids). These are thus considered as reliable smart materials for numerous engineering applications particularly where an adaptive response is desired from a rubber-like material such as adaptive tuned vibration absorbers [4, 5], adaptive vibration isolators [6-8], vehicle seat suspension [9, 10], engine mounts [11], adaptive beam structures [12], sensing devices [13] and MRE based actuators for valves [14].

MREs are composed of three fundamental components: ferromagnetic particles, elastomeric matrix and the additives. Compared to their fluid analogous (MR fluids), relatively larger sizes of polarizable particles could be used in MREs since the particles sedimentation is not a concern in MREs [15]. Research on the theories describing the magnetism of iron nanoparticles started by early 1960s [16], and has continued in earliest by development of new synthesis techniques for nanoparticles to improve their homogeneity, electrochemical and ecofriendly properties [17, 18]. The reported studies have widely employed different sizes of carbonyl iron particles (CIPs), ranging from 1μm to 200μm. Owing to their high saturation magnetization, the CIPs are considered well-suited for the MR materials [19, 20]. In order to achieve a higher MR effect, the particles must be large enough to support at least several magnetic domains. The MREs have been fabricated using different types of matrix materials such as silicone rubber, natural rubber, thermoplastic elastomers and polyurethane. Furthermore, additives are generally used to increase the fluidity and stability of the matrix [21]. Silicone oil is the most common additive in MRE fabrication, which works as a softening agent, and decreases the storage modulus of the elastomeric matrix. Additives also prevent the agglomeration of ferromagnetic particles, and increase the compatibility of the matrix with the particles [22]. Such added ingredients thus help achieve more uniform distribution of internal stress in the material, which makes the material properties more stable [21]. The fabrication process generally begins with thorough mixing of the three primary components (ferromagnetic particles, matrix material and additives) [4, 6]. The mixture is then vacuumed in a controlled environment in order to extract the air bubbles. Depending on the MRE type, the mixture is then permitted to cure in the absence (isotropic MRE) or presence of a magnetic field (anisotropic MRE). A strong magnetic flux, normally up to 1 T, is applied to realize anisotropic property of the MRE. While some silicone rubbers can be cured at room temperature, a constant temperature above 100℃ has been generally suggested to speed up the curing process. In order to achieve substantial MR effect from an isotropic MRE, the iron particle concentration has to be close to the critical particle volume concentration (CPVC), where the inter-particle distances are minimal. The pre-cure orientation of the particles in this case will not affect the absolute MR effect [23]. However, the composite with such high iron particle concentration exhibits high zero-field modulus, and thereby relatively lower relative MR effect. The softening of the matrix thus constitutes one of the challenges in MRE fabrication in order to achieve higher relative MR effect.

Reported studies have employed widely different matrix materials, volume fraction and sizes of ferromagnetic particles, and additive materials, apart from some variations in the fabrication method, which are summarized in Table 1 [2, 5, 8, 20, 24-42] in a chorological order. The table presents the matrix compound and iron particles considered in each study together with the particle content. From the review of these studies, it is evident that the vast majority of the studies have employed a blend of silicone rubber with silicone oil as the matrix compound and CIPs with average size ranging from 1 to 10 μm. Although the reported studies have focused on MREs with both the

isotropic and anisotropic property, the isotropic MREs have become more widespread since these do not require magnetic field during the curing process.

A few studies have evaluated dynamic responses of MREs considering different applications and excitations [6, 8, 43]. These have illustrated considerable challenges due to intrinsic hysteresis behavior and coupled nonlinear dependence on both the excitation condition and the magnetic field intensity. Although, the properties of MREs have been widely studied during the past decade using experimental and analytical methods, standardized methodologies for characterization and modeling of MREs do not yet exist. Reported studies have employed widely different methods and experimental conditions for characterizing the mechanical properties of MREs. They may be classified into two groups based on the operation mode, namely the uniaxial tension or compression and simple shear. The studies reporting characteristics of MREs in the shear mode may be further categorized into two groups. The first group of studies is aimed at characterization of MRE samples alone [20, 26, 30, 32, 34-38, 43, 44], while the second group of studies is focused on characterization of MRE-based devices such as vibration absorbers and isolators [2, 7]. Table 2 summarizes the range of loading conditions including the excitation frequency, strain amplitude as well as the magnetic flux density, considered in the first group of studies together with the sample dimensions and the test method. These have employed double-lap shear test methods and rheometry to characterize shear properties of the MREs. The studies using the double-lap shear method have employed widely different sizes of MRE samples, while those using rheometry have considered circular samples of the same size. The MRE hysteresis characteristics, whether in the stress-strain or in the force-displacement, however, have been reported in fewer studies [35, 36, 43].

The characterizations of MREs have been mostly limited to low frequency excitations and relatively low strain amplitudes. The characteristics of MREs subject to strain level exceeding 10% at frequencies above 5 Hz are thus not fully explored. Apart from the limited ranges of loading conditions, the studies are mostly focused on MRE samples with relatively low ferromagnetic particles content. The nonlinear behavior of the MRE, which may resemble that of the viscoelastic materials, is thus not fully explored. Moreover, the reported studies have employed widely different test methods for characterizing properties of MREs. In the present study, the static and dynamic characterizations of MREs were performed in accordance with the available standardized methods for rubbery type materials under wide ranges of strain amplitudes and excitation frequencies. Isotropic MREs with different ferromagnetic particles content and matrix material were fabricated in the laboratory, and effects of the constituents on the magneto-mechanical properties were investigated, namely, the zero-field shear modulus, and relative and absolute MR effects. The static characteristics of the MRE samples, obtained using the standardized double-lap shear test, revealed substantially higher MR effect of the sample with higher volume fraction of iron particles. The dynamic characterizations of the sample with enhanced MR effect were subsequently performed under shear strain ranging from 2.5 to 20% in the 0.1 to 50 Hz frequency range, and varying magnetic flux density (0-450 mT). The measured data are used to determine dynamic properties of the MRE in terms of elastic and loss shear moduli (G', G''), and their dependency on the loading conditions as well as the applied magnetic flux density.

Table 1: The matrix compound and iron particles content used in MRE samples fabricated in selected reported studies.

Study	Matrix	Particles	Particle content	Type of MRE
Shiga [24], 1995	Silicone gel	Iron (100μm)	Up to 28% Vol	Anisotropic
Jolly et al. [19], 1996	Silicone oil	CIP (3-4μm)	10 to 30% Vol	Anisotropic
Ginder et al. [26], 1999	Natural rubber	CIP (0.5-5μm)	27 and 40% Vol	Isotropic & Anisotropic
Bellan et al. [27], 2002	Silicone rubber; Silicone oil	CIP (2μm) Nickel particles	5 to 25% Vol	Anisotropic
Lokander and Stenberg [20], 2003	Nitrile rubbers acrylonitrile	large & irregular shaped pure iron particles (60,180, 200μm); and CIP (3.9-5μm)	-	Isotropic
Farshad et al. [28], 2004	Silicone rubber	CIP (3.8μm)	27% Vol	Anisotropic
Kallio et al. [29], 2005	Natural rubber Silicone rubber Thermoplastics	CIP (4μm); and Irregular iron particles (up to 200μm)	-	Anisotropic
Gong et al. [30], 2005	Silicone Rubber; Silicone oil	CIP (3μm)	20 to 70% Weight	Isotropic
Lockette et al. [31], 2006	Silicone rubber	combination of 40μm and 10μm iron particles	Up to 32% Vol	Anisotropic
Stepanov et al. [32], 2007	Silicone rubber	Combination of 2-4μm and 2-70μm Iron particles	30 to 37% Vol	Isotropic Anisotropic
Lerner et al. [33], 2007	Silicone rubber	CIP (6-9μm)	Up to 35% Vol	Anisotropic
Böse et al. [34], 2009	Silicone rubber	CIP (5μm) CIP (40μm)	0 to 35% Vol	Isotropic & Anisotropic
Jung et al. [35], 2009	Silicone rubber	Iron particles (10μm)	30% Vol	Isotropic
Li et al. [36], 2010	Silicone rubber; silicone oil	CIP (5μm)	60% weight	Anisotropic
Danas et al. [37], 2011	Natural rubber	CIP (0.5-5μm)	25% Vol	Anisotropic
Gordaninezhad et al. [38], 2012	Silicone elastomer	CIP (2-8 μm)	30 to 70% weight	Anisotropic
Li et al. [39], 2013	$^{+}$RTV Silicone Rubber	5μm	30% Vol	Anisotropic
Li et al. [8], 2013	Silicone Rubber; Silicone Oil	CIP (3-5μm)	23% Vol	Isotropic
Agirre-Olabide et al. [40], 2014	Silicone rubber; Vulcanizer	CIP (1.25±0.55μm)	10 to 30% Vol	Isotropic & Anisotropic
Sun et al. [2, 5, 41], 2014-2015	Silicone Rubber; Silicone oil	CIP (3-5μm)	75 to 80% weight	Isotropic

Yu et al. [42], 2016	Silicone rubber; Silicone Rubber	CIP (3-5μm)	23% Vol	Isotropic
Vatandoost et al. [22], 2017	Silicone rubber; Silicone oil	CIP (3-5μm)	70% Weight	Isotropic
Wan et al. [45], 2018	Silicone rubber	CIP (5-9μm)	30% Vol	Anisotropic

[+] RTV, Room-Temperature-Vulcanizing.

Table 2: Summary of test methods and conditions employed for characterizations of MREs samples in the reported studies.

Authors - Year	**Sample shape/dimensions** ***Test method***	**Frequency range**	**Amplitude range**	**Magnetic flux density**
Ginder et al. [26]	Disc-shaped specimens *Double-lap shear*	2 Hz	1.5, 3, 6%	Up to 1500 mT
Lokander and Stenberg [20]	$20 \times 15 \times 2\ mm^3$ *Double-lap shear*	2.5% at 1 Hz decreased with increasing frequency to 0.6% at 21 Hz		170 kA/m ($\approx 214\ mT$)
Gong et al. [30]	$6 \times 10 \times 30\ mm^3$ *Single Shear*	100 - 600 Hz (Random)	Not Reported	0 and 200 mT
Stepanov et al. [32]	$10 \times 10 \times 5\ mm^3$ *Double-lap shear*	Static	Up to 30% shear strain at 0mT, Up to 15% shear strain at 80mT	Up to 80mT
	Circular (*d = 20mm, *t = 1mm) *Rheometery*	Up to 5 Hz	Not Reported	30~70 mT
Bose and Roder [34]	- *Rheometery*	10 Hz	1%	Up to 700 mT
Jung et al. [35]	$19.05 \times 12.7 \times 12.7\ mm^3$ Double-Lap shear	0.1 to 3 Hz	1.0, 3, 5 mm displacement	50~500 mT
Popp et al. [44]	Circular (*d = 20mm, *t =1mm) *Rheometery*	up to 100 Hz (sweep)	0.1, 1, 5, 10, 15%	409 mT
Li et al. [36]	Circular (*d = 20mm, *t =1mm) *Rheometery*	1, 5 and 10 Hz	1, 5, 10, 50%	Up to 750 mT
Danas et al. [37]	$24 \times 12 \times 12\ mm^3$ *Double-lap shear*	Static	Up to 15%	Up to non-dimensional magnetic field = $h/\rho_0 M_s = 1$
Gordaninezhad et al. [38]	$22.45 \times 12.7 \times (6.35, 12.7, 19.05, 25.4)\ mm^3$ *Double-lap shear*	Static	0.1 to 10%	0, 590 and 990 mT
Norouzi et al. [43]	$50 \times 12 \times 9.5\ mm^3$ Double-lap	0.1 to 5 Hz	2, 4, 8, 16%	100 to 272 mT
Jung et al. [46]	Circular (*d = 20mm, *t =1.2 mm) *Rheometery*	1 Hz	0.01 to 5% (sweep)	Up to 343 kA/m ($\approx 430\ mT$)
		1 to 100 rad/s (0.16 to 15.9 Hz) (sweep)	0.02 %	

* d = diameter; t = thickness

2. Fabrication and Experimental Method

Six different types of MRE samples were fabricated in the laboratory with varying volume fractions of the ferromagnetic particles and the matrix material, as summarized in Table 3. Spherical carbonyl iron particles (BASF-SQ) with diameter ranging from 3.9 to 5 μm were dispersed into the matrix material, which was chosen as a silicone rubber (Eco-Flex Series, Smooth-on, Inc.). Furthermore, two additives were used, including the slacker (Smooth-on, Inc.) as the softening agent and the silicone thinner (Smooth-on, Inc.) as the diluting agent. According to the manufacturer's (Smooth-on, Inc) guidelines, slacker changes the feel of the silicone rubber to a softer material, while the silicone thinner lowers the mixed viscosity of silicone rubber products [47]. The mixture was used to fabricate the MRE samples using the methods reported in [4, 6]. Briefly, the process was initiated by computing the desired weight fractions of each component, which was followed by thorough mixing of all the ingredients in a container using an electrical blender for nearly 5 minutes. The mixture was then placed in a vacuum chamber for 5 minutes under 29 in-Hg pressure. The grey blend was subsequently poured in circular molds (100mm diameter - 10 & 5mm thick), and cured for 20 minutes at a temperature of about 65°C. Six different types of samples, listed in Table 3, are denoted as *Type 1* to *Type 6*. Apart from the CIP and matrix material fractions, the fabrication process involved variations in the slacker and thinner contents. *Type 1* to *Type 3* samples were fabricated without the additives, while only softening agent was used for *Type 4* and *Type 5* samples. The *Type 6* sample included both the softening and the diluting agents (slacker and silicon thinner). The use of additives was essential for mixing of uncured blends for *Type 5* and *Type 6* MRE samples due to their greater CIP content (30 and 40% volume fraction). The reason for using 10% silicone thinner for MRE sample type 6 is to bring the viscosity of the whole mixture to a lower value, otherwise it was not possible to thoroughly mix the iron particles with the silicone rubber and slacker due to high viscosity of the mixture. Figure 1 illustrates a typical MRE sample fabricated in the laboratory.

Table 3: The volume fraction of the constituents used in different types of MREs.

MRE sample	**Volume fractions of constituents**			
	CIP	Silicone rubber	Slacker	Silicone thinner
Type 1	12.5	87.5	-	-
Type 2	17.5	82.5	-	-
Type 3	25	75	-	-
Type 4	25	60	15	-
Type 5	30	50	20	-
Type 6	40	40	10	10

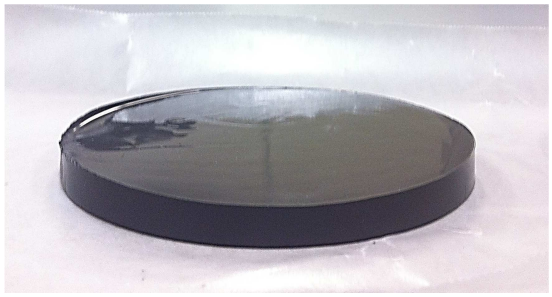

Figure 1: A pictorial view of a MRE sample.

2.1 Experimental Setup and Methods

Two series of experiments were designed for characterization of static and dynamic properties of the MRE samples in the shear mode. The experimental methods were formulated on the basis of standardized test methods defined in ISO-1827 [48] and ISO-4664 [49] for characterizations under static and dynamic conditions, respectively. The experiments under dynamic conditions were designed to include relatively broad ranges of strain as well as excitation frequencies in order to obtain dynamic characteristics of the MRE over a wide spectrum of loading conditions. The methods and the experimental setup designed in the study are described below.

A double-lap test setup was designed to characterize the stress-strain properties of MREs in the shear mode under both static as well as dynamic conditions. The shear loading fixture was constructed via 3D printing of a very stiff polymer, Bio-Flex V 135001. Rectangular specimens ($25mm \times 20mm \times 5mm$) of each types of MRE were prepared for the static and dynamic tests, as recommended in ISO-1827 [42]. The test specimen was sandwiched between the inner and outer members of the double-lap shear test fixture, as shown in Figure 2. The experiments were conducted using the table top Bose ElectroForce 3200 test system in the displacement control mode. The test fixture with the specimen was attached to the test system via two non-magnetic material shafts. The upper shaft, fixed to the actuator, was attached to the inner member of the fixture. The lower shaft attached to the outer member of the fixture was attached to the fixed base via a load cell. Neodymium permanent magnets were used to generate the desired magnetic flux density. Two sets of permanent magnets (50mm×50mm×10mm each) were positioned symmetrically about the central axis of the test arrangement so as to apply the magnetic field in the thickness direction of the specimens, as shown in Figure 3. The fixture holding the permanent magnets was designed so as to permit variations in the distance between the magnets and the fixture containing the specimen. This permitted variation in the density of the magnetic flux imposed on the MRE specimen. The use of non-magnetic material for the dual-lap fixture and the shafts ensured minimal magnetic field leakage. The magnetic flux density was measured in the vicinity of specimen's thickness center using a Gauss-meter, which was, about 5 mm from the line of symmetry of the test fixture, as shown in Figure 3. Figure 4 illustrates variations in the magnetic flux density measured at the distance of 5 mm from the line of symmetry considering six different distances between the magnets, ranging from 25 to 75 mm. The measured data suggest that the magnetic flux density decreases exponentially with increasing distance between the magnets. The results further suggest that the test setup could

provide static and dynamic characterization of the MRE specimens under magnetic flux density in the 150 to 450 mT range.

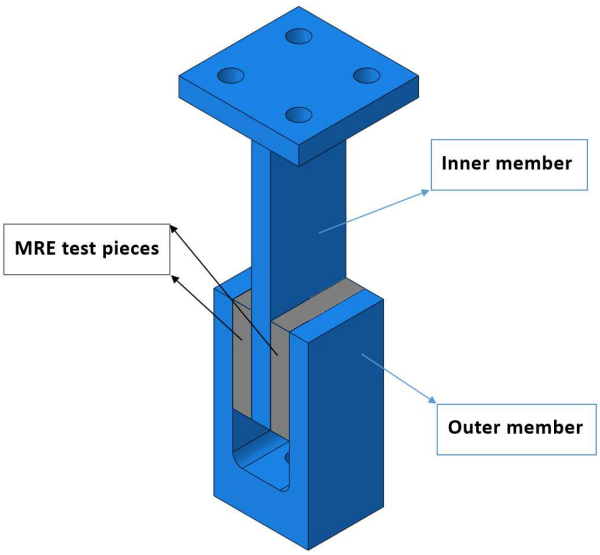

Figure 2: Dual-lap shear test fixture with MRE specimens.

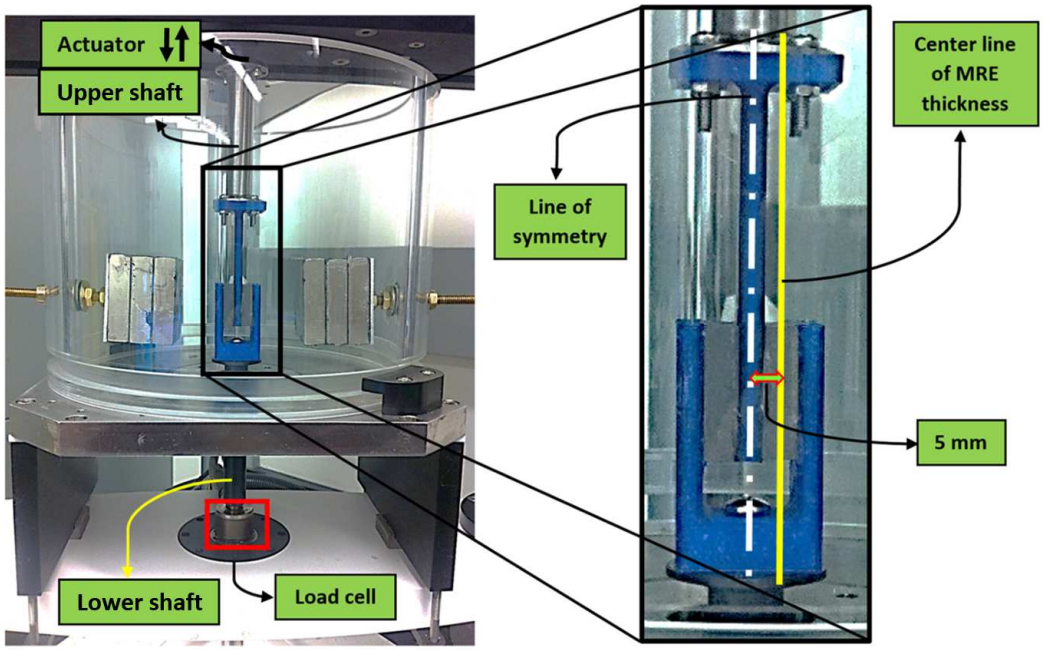

Figure 3: Double-lap shear test set-up fixed within the Bose ElectroForce test system and arrangement of permanent magnets.

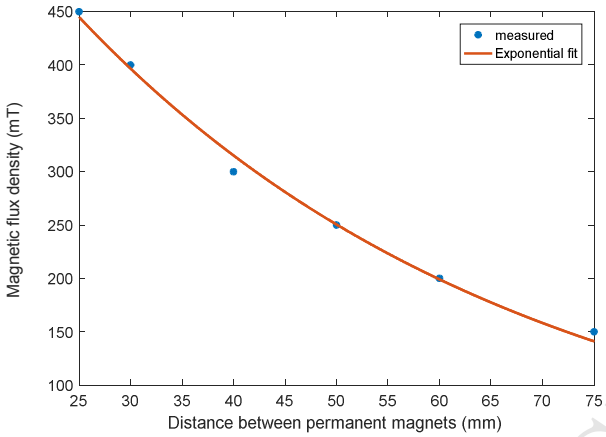

Figure 4: Variations in the magnetic flux density measured near the center of the MRE specimen thickness with distance between the permanent magnets.

2.1 Static Characterization

Static tests were performed in accordance with ISO-1827 [42] by applying static shear deformation to the specimen via the inner member. The deformation was applied in a ramp manner at a rate of 5 mm/min to achieve maximum shear strain of 30%. This corresponds to peak deformations of 1.5 mm of the 5 mm thick MRE specimens. The deformation was measured using the displacement sensor, integrated within the test system, with resolution of $1\mu m$. Both the displacement and force signals were acquired at a sampling rate of 2000 Hz. The data were acquired under three different intensities of the applied magnetic flux (150, 300 and 450 mT), which were achieved by selecting the distance between the permanent magnets as 75mm, 40mm and 25mm, respectively. The experiments with each specimen were performed under deformations in the upward as well as downward directions. Furthermore, each measurement was repeated two times.

Owing to the symmetric nature of the test arrangement, no noticeable difference was observed between the tests results obtained under deformations in the upward and downward directions. The data acquired during 4 trials for each specimen were thus averaged for characterizing the mean stress-strain characteristics of the specimens. The mean static shear modulus of six different MRE samples considered in the study were subsequently computed using the method described in ISO-1827 [42]. The mean shear moduli of different types of MR samples are further analyzed to obtain their respective absolute as well as relative MR effects. The absolute MR effect is defined by difference between the shear moduli measured under the maximum (450 mT) and minimum (0 mT) magnetic flux density. The ratio of this absolute change to the modulus obtained in the absence of the magnetic field provided the relative MR effect of the each type of sample.

2.2 Dynamic Characterization

The measurements of dynamic characteristics were limited to the MRE exhibiting greatest MR effect, which was observed for the sample with highest fraction of carbonyl iron particles. (*Type 6*). The reported studies have shown important effects of excitation frequency and deformation amplitude on dynamic properties of MREs apart from the

magnetic flux density. The vast majority have been limited to low frequencies up to only 10 Hz or low strain amplitudes (Table 2). Gong et al. [27] characterized an MRE under single-shear and random excitation in the 100-600 Hz, while the magnitude of excitation was not stated. Popp et al. [41] investigated dynamic properties of a circular MRE using rheometry under excitations swept up to 100 Hz. The study, however, considered a very thin MRE sample (1mm). The experiment in this study was designed to characterize the sample properties over wide ranges of harmonic strain amplitude and frequency, and flux density. The measurements were performed under four different amplitudes of harmonic strain (2.5, 5, 10 and 20%), each being applied at four different frequencies (0.1, 1, 10 and 50 Hz). Measurements under each input were also performed under four different densities of the magnetic flux, namely, 0, 150, 300 and 450 mT. The experiment design thus resulted in a total of 64 measurements. The force and displacement signals were acquired during each measurement, while the sampling rate was adjusted to achieve a total of 100 measurements per cycle, irrespective of the excitation frequency. The measured data were analyzed to describe shear stress - shear strain characteristics of the sample as functions of the three inputs, namely, strain amplitude, frequency, and magnetic flux density. The data in the steady state alone are considered to describe hysteresis in the stress-strain loops. The dynamic properties of the MRE sample such as storage (elastic) and loss moduli are further quantified from the stress-strain hysteresis loops using the method described in ISO 4664 [49].

4. Results and Discussions

4.1. Static characteristics of the MRE samples

Figure 5 illustrates mean shear stress-shear strain properties of the MRE samples (*types 1* to *6*) obtained from the static tests considering four different magnetic flux densities. The results show increasing stiffness of the samples with increasing magnetic flux density, which has also been reported in [39, 50]. The mean measured data show nearly linear stress-strain behavior of the MREs in the absence of the magnetic field, similar to that of the filled rubbers [51]. The nonlinearity in the stress-strain relationship is apparent under the applied magnetic field, which is more pronounced under the higher magnetic flux of 450 mT for all the samples. This nonlinearity is further compounded by increase in the volume fraction of iron particles, which is more evident for *types 4*, *5* and *6* samples (Table 3). Under lower strain excitations (below 5%), the slopes of stress-strain curves tend to decrease and approach to nearly constant values with further increase in the strain. The gradual decrease in the slope of the strain-stress curve has been related to strain softening characteristic of filled rubbers [36, 51]. The higher magnetic flux densities, however, show a significant reduction in the slope, which is clearly evident for all types under the 450 mT field density. This trend has been attributed to weakening of the dipoles network due to greater distances between the adjacent iron particles under increasing strain [32, 36]. This effect is more noticeable for MRE samples (*types 4*, *5* and *6*) with higher fraction of iron particles under exposure to higher magnetic flux density. The data obtained for the *Type 6* sample also exhibit increase in the slope of stress-train curve under strain amplitudes exceeding 20% and magnetic field densities of 300 and 450 mT. This trend was also noted in the data for other types, although the change in slope was very small. Such strain stiffening effect under large strain deformation has also been reported in a few studies focused on dynamic behavior of the MREs [7, 22]. This strain stiffening effect has also been attributed

to limited extensibility or saturation of the polymer chains [52], which contributes to increase in the shear modulus of the polymer.

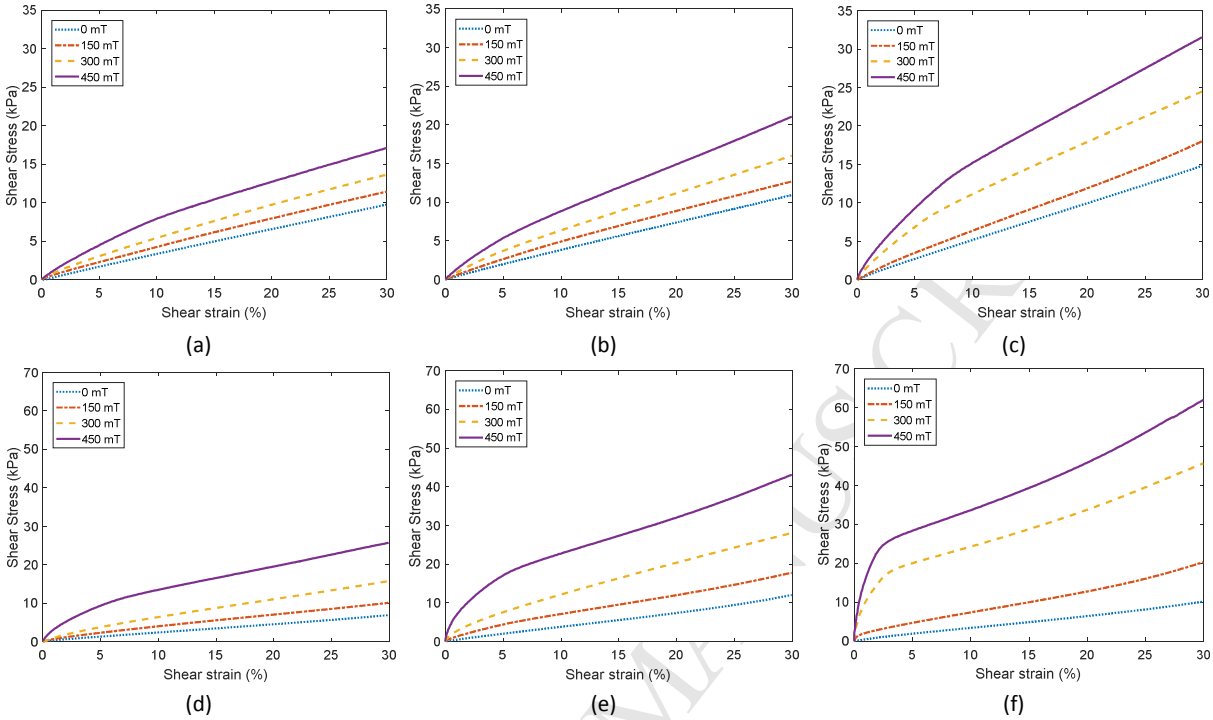

Figure 5: Stress-strain characteristics of MRE samples under different levels of magnetic flux density: (a) *Type 1*; (b) *Type 2*; (c) *Type 3*; (d) *Type 4*; (e) *Type 5*; and (f) *Type 6*.

The average static shear moduli of the MREs are further evaluated for different magnetic flux densities using the method described in ISO-1827 [48]. The standard defines the shear modulus as the ratio of shear stress to shear strain corresponding to 25% strain. Figure 6 shows variations in the shear moduli of all the MRE samples with magnetic flux density ranging from 0 mT to 450 mT. While the mean static shear modulus of all the samples increased with the applied flux density, the MRE with greatest concentration of iron particles (*type 6* - 40%) exhibits highest static shear modulus in the presence of the magnetic field. The results also suggest saturation of the shear modulus of MRE *type 6* under magnetic flux density exceeding 300 mT. Similar tendency has also been reported in [19, 53].

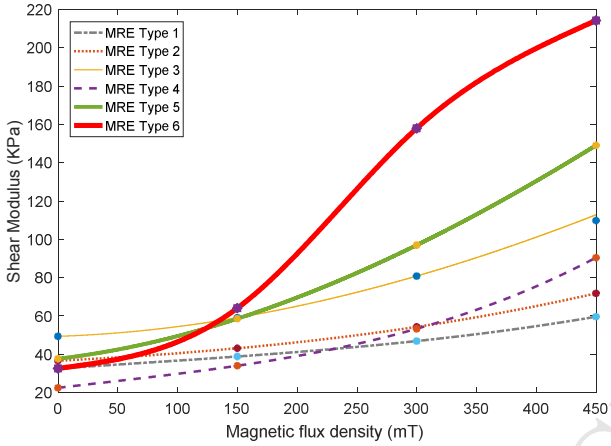

Figure 6: Variations in mean static shear modulus of MRE samples (*type 1* to *type 6*) with the magnetic flux density.

The measured stress-strain data are further evaluated in terms of zero-field shear modulus, shear modulus corresponding to the maximum magnetic flux density, and relative and absolute MR effect. Results, summarized in Table 4, are used to evaluate relative effects of the constituents on static properties of the MREs fabricated in the study. The effect of CIP fraction alone can be evaluated from the properties of *type 1*, *2* and *3* samples with CIP volume fractions of 12.5%, 17.5% and 25%, respectively. The results suggest that increasing the CIP volume fraction yields slight increase in the zero-field shear modulus but substantially higher modulus under 450 mT flux, and absolute and relative MR effect. This is likely due to stronger dipoles network of the elastomer with higher CIP concentration. The absolute MR effect increases nearly linearly with the CIP volume fraction. Increasing the CIP volume fraction from 12.5% to 25% yields over 100% increase in the absolute MR effect. The corresponding increase in the relative MR effect, however, is smaller, which is due to higher zero-field shear modulus for the higher CIP fraction.

Table 4: Static magneto-mechanical properties of the fabricated MREs

MRE *type*	Iron particles content (%)	Zero-field shear modulus (kPa)	Shear modulus at 450 mT (kPa)	Absolute MR effect (kPa)	Relative MR effect (%)
1	12.5	32.62	59.64	27.01	82.80
2	17.5	36.67	71.83	35.16	95.90
3	25	49.40	109.84	60.43	122.31
4	25	22.53	90.47	67.93	301.41
5	30	37.72	149.07	111.34	295.15
6	40	32.66	214.21	181.54	555.74

Comparisons of properties of *type 3* and *type 4* MREs show the effect of the softening agent since both types use identical CIP content (25%). *Type 4* MRE was realized by adding slacker (15% volume fraction) to the matrix material. The results suggest that addition of the softening agent reduces the zero-field shear modulus considerably, which is less than one-half of that of *type 3*. The softening also yields about 17% reduction in the maximum shear modulus when compared to that of *type 3*, while its and absolute MR effect increases by about 10%. The relative MR effect, however, increases to about 301% from 122% for *type 3* with the addition of the softening agent, which is due to significantly lower zero-field shear modulus of the type 4 MRE. Moreover, this may be attributed to the

fact that the slacker (softening agent) prevents localized accumulation of iron particles and facilitates frictional sliding at the interface between the matrix and the particles [22].

Type 5 MRE contains 30% volume fraction of CIP in addition to the slacker (20% volume fraction). The CIP concentration of 30% is close to the critical particle volume concentration (CPVC), defined as the ratio of the apparent density to the balk density of CIP, which is reported to be 29.1% for BASF SQ - carbonyl iron powder [29]. In this case, the particles may be in physical contact with each other, although it may yield maximum relative MR effect [29]. While the CIP concentration of *type 5* is only 5% greater than that of type 4, it exhibits nearly 68% and 63% higher values of the zero-field shear modulus, and absolute MR effect, respectively, compared to the *type 4*. The relative MR effect of both types, however, is quite comparable, which is due to higher zero-filed shear modulus of MRE *type 5*. This suggests that the relative MR effect may not necessarily approach the maximum when CIP concentration is close to the CPVC. Greater relative MR effect can be obtained by softening the matrix during the fabrication process.

The results obtained for *type 6* MRE are compared with those of *types 4* and *5* to identify the effects of silicon thinner on the static properties. It should be noted that the *type 6* MRE is composed of 40% CIP, 40 % silicone rubber, 10 % slacker and 10 % silicone thinner (all fractions are by volumes, as listed in Table 3). The results show nearly 13% reduction in the zero-field shear modulus of *type 6* compared to *type 5*, while its maximum modulus under 450 mT flux density is nearly 120% of that of *type 5*. The *type 6* MRE yields the highest absolute (181.54 kPa) absolute and relative (555.74%) MR effects amongst all the MRE types considered in the study. Higher relative MR effect cannot be entirely attributed to its lower zero-field shear modulus, which is either comparable or higher than those *types 1* and *4*. The results suggest that both the maximum shear modulus and the relative MR effect of an MRE can be significantly enhanced by increasing the particle volume fraction beyond the critical value, provided that an adequate level of a softening agent is used to limit the zero-field shear modulus. Such an MRE can yield wider control bandwidth in view of the elastic and loss modulus properties.

4.2. Dynamic characteristics of the MRE samples

The dynamic characterizations were performed with *type 6* MRE alone, which revealed highest absolute and relative MR effects. The measured data are analyzed to study the influences of excitation frequency, strain amplitude and magnetic flux density on the stress-strain properties, complex shear modulus and hysteresis. The elastic and loss shear moduli of the MRE are further evaluated using the method described in ISO-4664 [49].

4.2.1 Effect of excitation frequency

The measured data revealed important effects of excitation frequencies on the stress-strain characteristics of the MRE, especially on the hysteresis. As an example, Figure 7 illustrates the stress-strain characteristics measured under 10% shear strain at different frequencies in the 0-50 Hz frequency range. The results also show the effect of magnetic flux density. Nearly visco-elastic behavior, similar to that of a filled rubber, is observed in the absence of the magnetic field. The slope and hysteresis of the stress-strain loops increase considerably with increasing

frequency under 0 and 150 mT flux density, as seen in Figs. 7(a) and 7(b), suggesting strong dependence of effective stiffness and damping of the MRE. This frequency dependence of the stress-strain characteristics, however, tends to saturate under higher magnetic flux densities, as seen in Figs. 7(c) and 7(d). The results also show that perfectly elliptic hysteresis loops, obtained in the absence of the magnetic field, transform to non-elliptical loops with the applied magnetic field. This nonlinear tendency is more apparent under 300 and 450 mT flux density, which is attributed to the strain softening effect, as observed in static stress-strain properties of *type 6* MRE in Fig. 5(f).

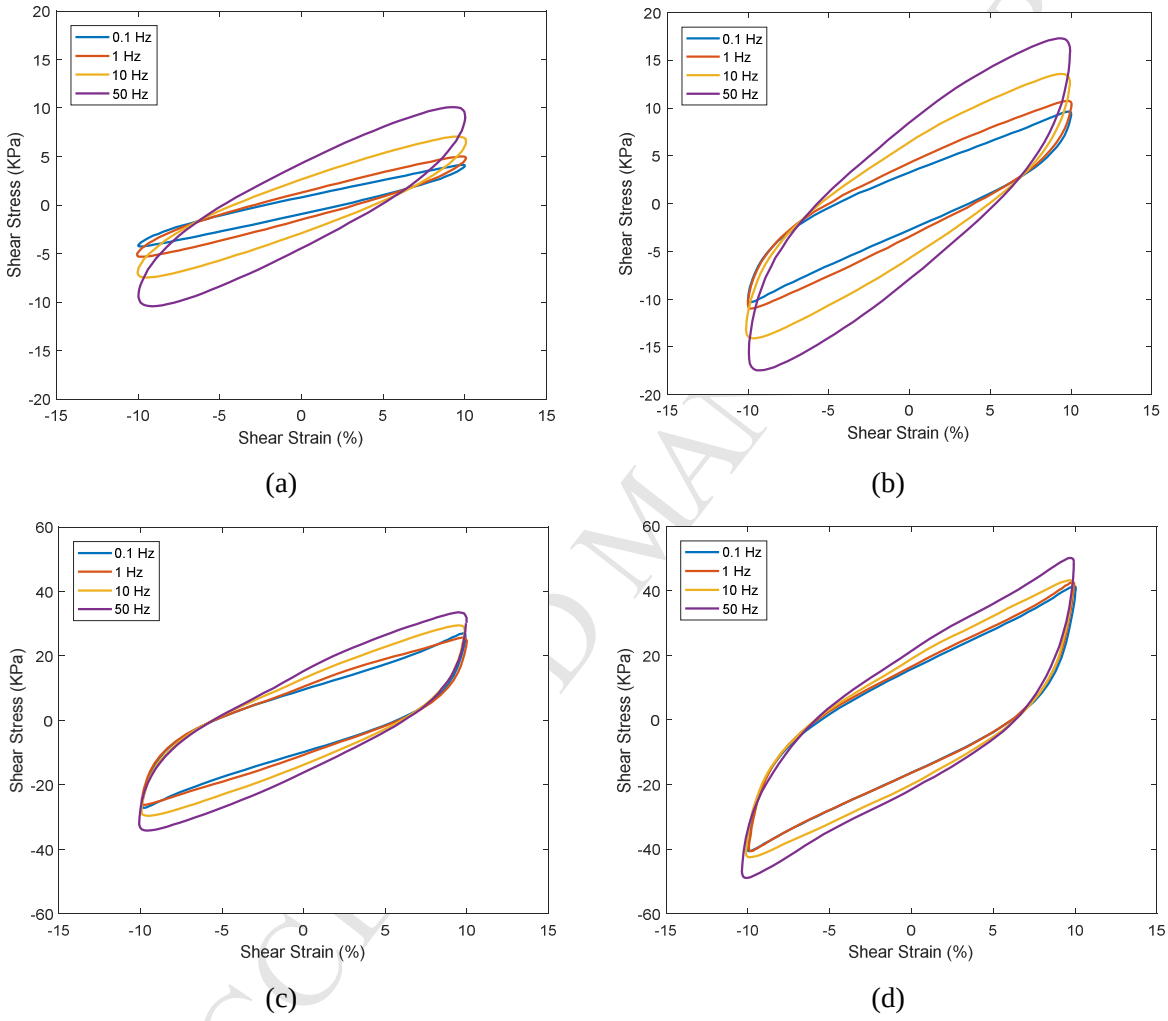

Figure 7: Excitation frequency dependence of stress- strain characteristics of MRE (*type 6*) measured under 10% shear strain and different levels of magnetic flux density: (a) 0mT; (b) 150mT; (c) 300mT; and (d) 450mT.

The frequency dependence of the stress-stress characteristics yields significant effect of the excitation frequency on the elastic and shear moduli of the MRE, as seen in Figs. 8 and 9, respectively. The results are presented for different magnitudes shear strain and flux density. Both the moduli increase with increasing frequency in a nearly exponential manner under 0 mT or lower flux density (150 mT), irrespective of the strain amplitude. The observed strain rate stiffening effect is similar to that reported for filled rubbers [54]. Both the moduli increase substantially with increase in the strain and the flux density. The dependency of the moduli on the excitation frequency, however,

diminishes with increasing magnetic field, as seen in Figs. 8(c), 8(d), 9(c) and 9(d). This is likely due to saturation of the MRE under higher magnetic flux density, as observed in the measured stress-stress data in Fig. 7. The MRE exposed to higher magnetic field yields relatively higher increase in the loss modulus compared to the storage modulus, irrespective of the strain amplitude. For instance, the loss modulus of the MRE under and 0 mT flux and 2.5% strain increases from 11.95 kPa to 60.75 kPa (≈408%), when the frequency is increased from 0 to 50 Hz. The corresponding increase under 450 mT flux density is only 33.74% (392.7 kPa to 525.2 kPa), although the increase is quite considerable.

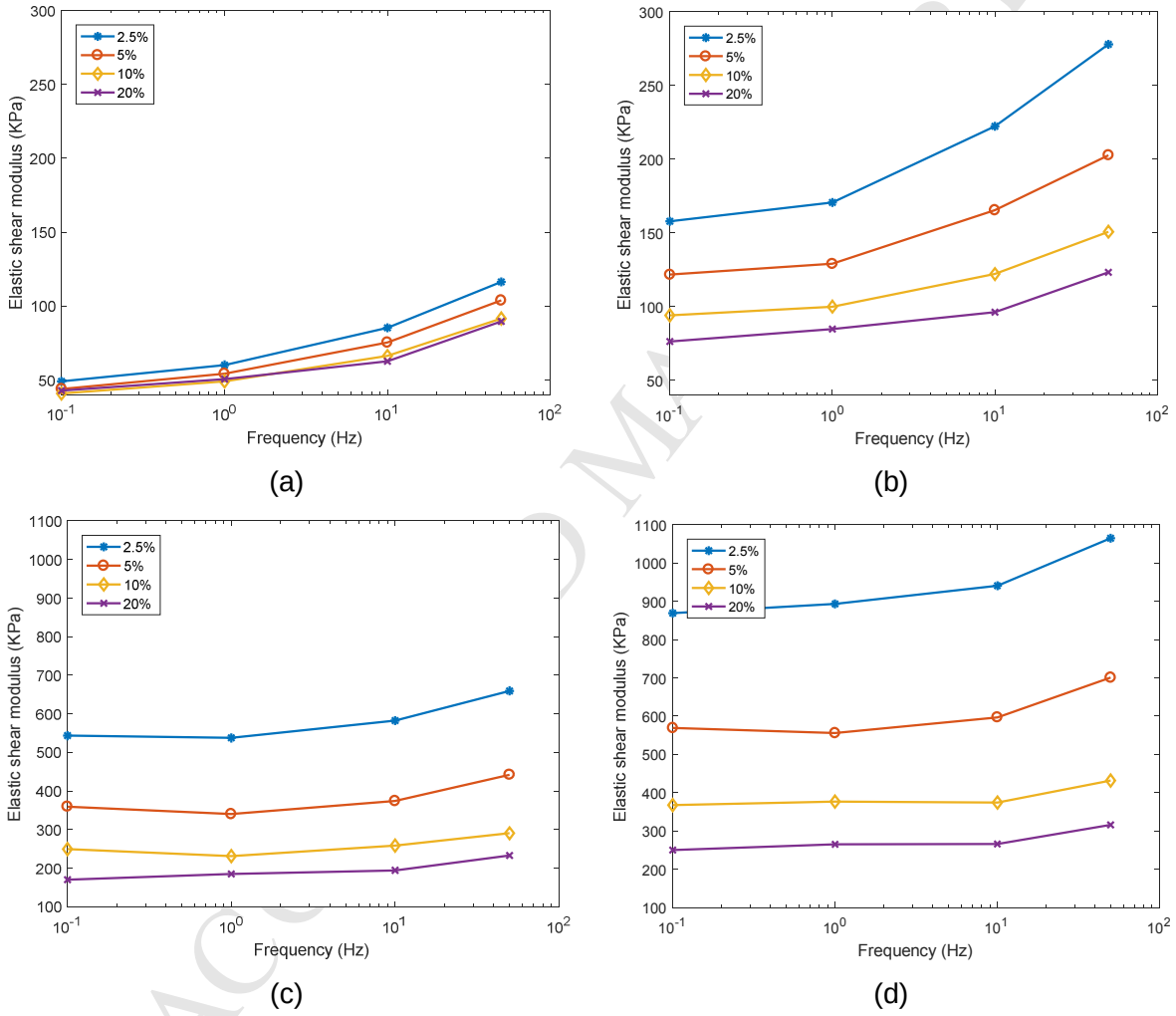

Figure 8: Effects of excitation frequency on elastic shear modulus of the MRE subject to different strain amplitudes and magnetic flux density: (a) 0mT; (b) 150mT; (c) 300mT; and (d) 450mT.

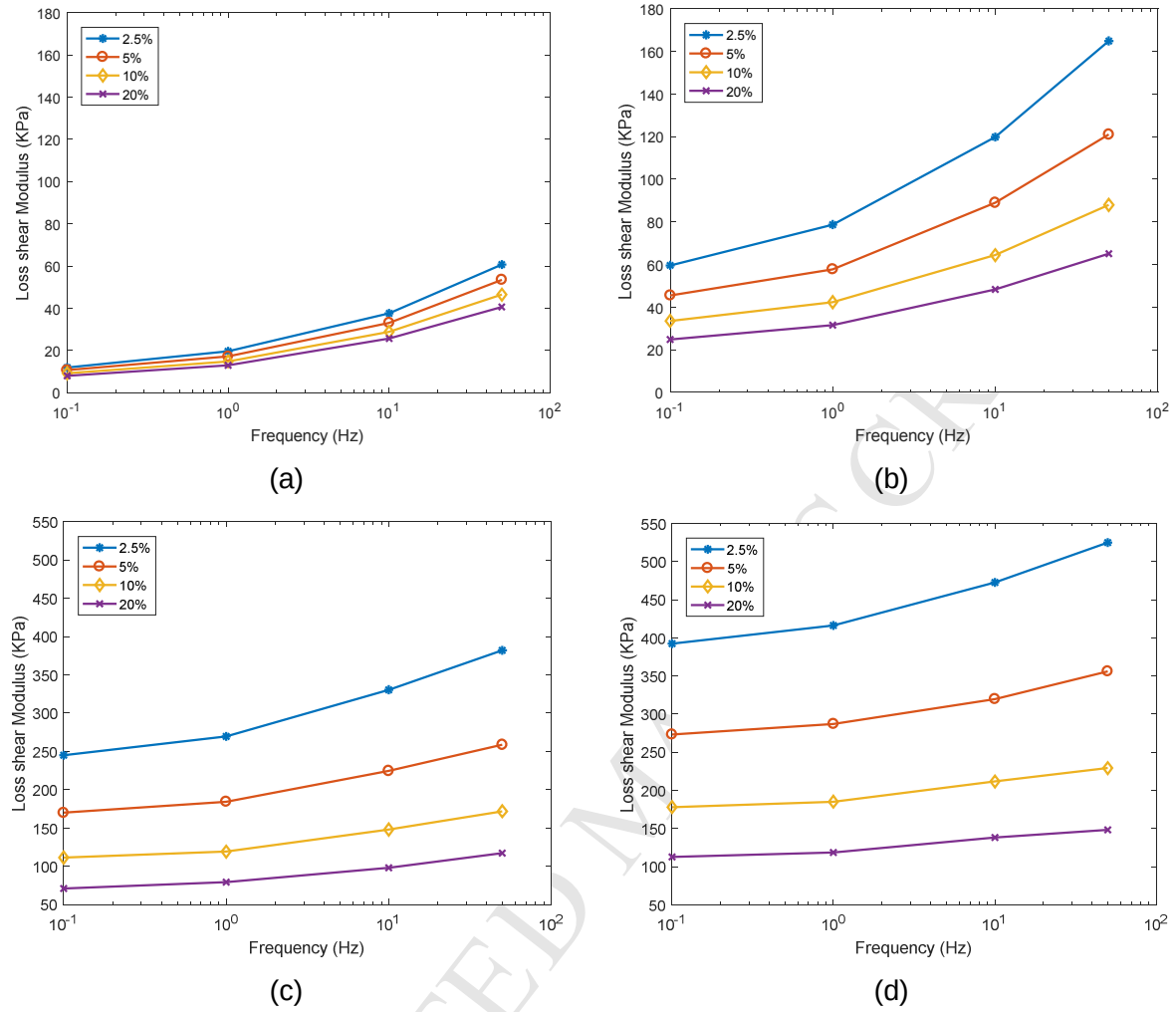

Figure 9: Effects of excitation frequency on loss shear modulus of the MRE subject to different strain amplitudes and magnetic flux density: (a) 0mT; (b) 150mT; (c) 300mT; and (d) 450mT.

4.2.2 Effect of strain amplitude

Increase in the strain amplitude yields substantially lower storage and loss moduli, especially in the presence of a magnetic flux, irrespective of the excitation frequency and flux density, as seen in Figs. 8 and 19. The significant effects are further evident from the stress-strain characteristics, shown in Figure 10, in terms of slope and hysteresis. The results are presented considering the excitation frequency of 10 Hz and different magnetic flux densities. The slope of the hysteresis loop, representing the storage modulus of the MRE, decreases substantially with increase in the strain amplitude. This tendency is more pronounced under higher magnetic flux density. Moreover, the hysteresis loops under low strain amplitudes are nearly elliptic and transform to non-elliptical shape under higher strain amplitudes. This suggests that the MRE behaves like a nonlinear viscoelastic material under high strain amplitudes and flux density, irrespective of the excitation frequency. Under lower applied magnetic field (150 mT), the transition from linear to nonlinear behavior occurs at relatively higher strain amplitude (above 5%), while it is observed around the low strain (2.5%) under the higher flux density of 450 mT.

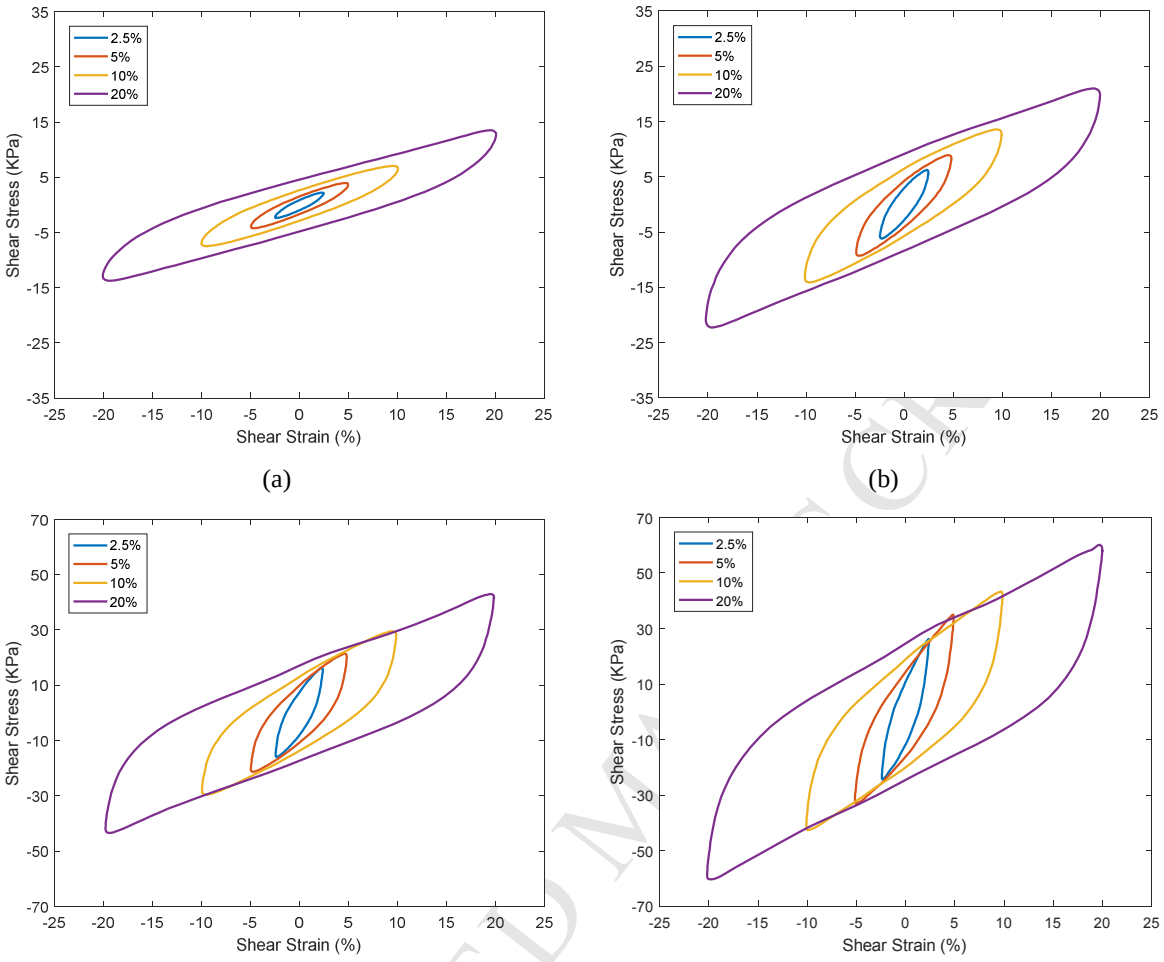

Figure 10: Effect of strain amplitude on the measured stress-strain characteristics of the MRE in simple shear mode at 10 Hz and different magnetic flux density: (a) 0mT; (b) 150mT; (c) 300mT; and (d) 450mT.

The effect of variations in strain amplitude on the elastic and loss shear moduli of the MRE are illustrated in Figs. 11 and 12, respectively, considering different excitation frequencies and magnetic flux densities. The results clearly show that both the moduli decrease with increase in the strain amplitude in an exponential manner, especially in the presence of the magnetic flux. As expected, it is observed that the elastic shear modulus decreases by increasing the amplitude of excitation. The rate of decrease in the moduli, however, tends to be lower under strain amplitudes exceeding 10%. Moreover, the strain amplitude dependence of the elastic and loss shear moduli is notably higher under higher magnetic flux density.

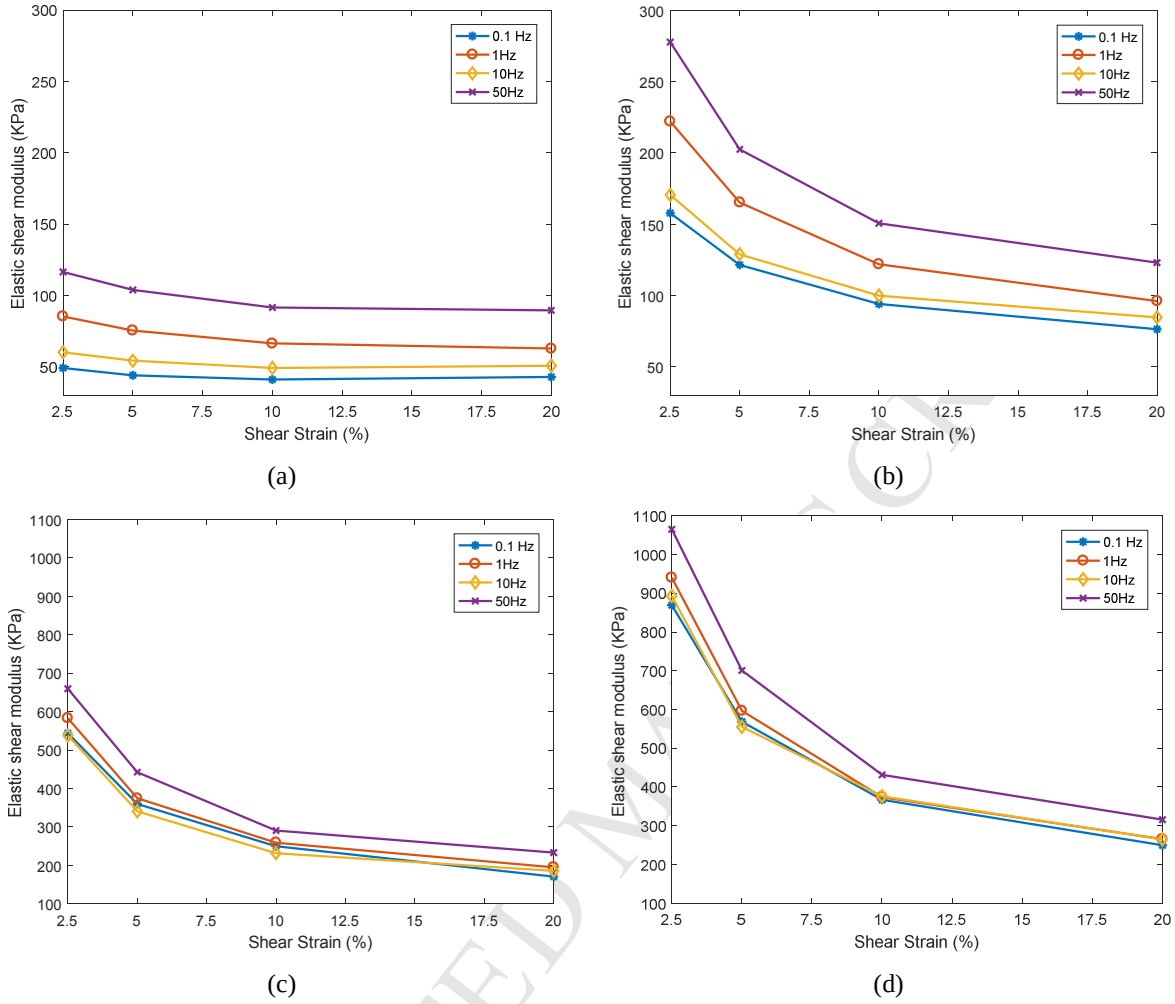

Figure 11: Effect of strain amplitude on the elastic shear modulus of the MRE at different excitation frequencies and levels of magnetic flux density: (a) 0mT; (b) 150mT; (c) 300mT; and (d) 450mT.

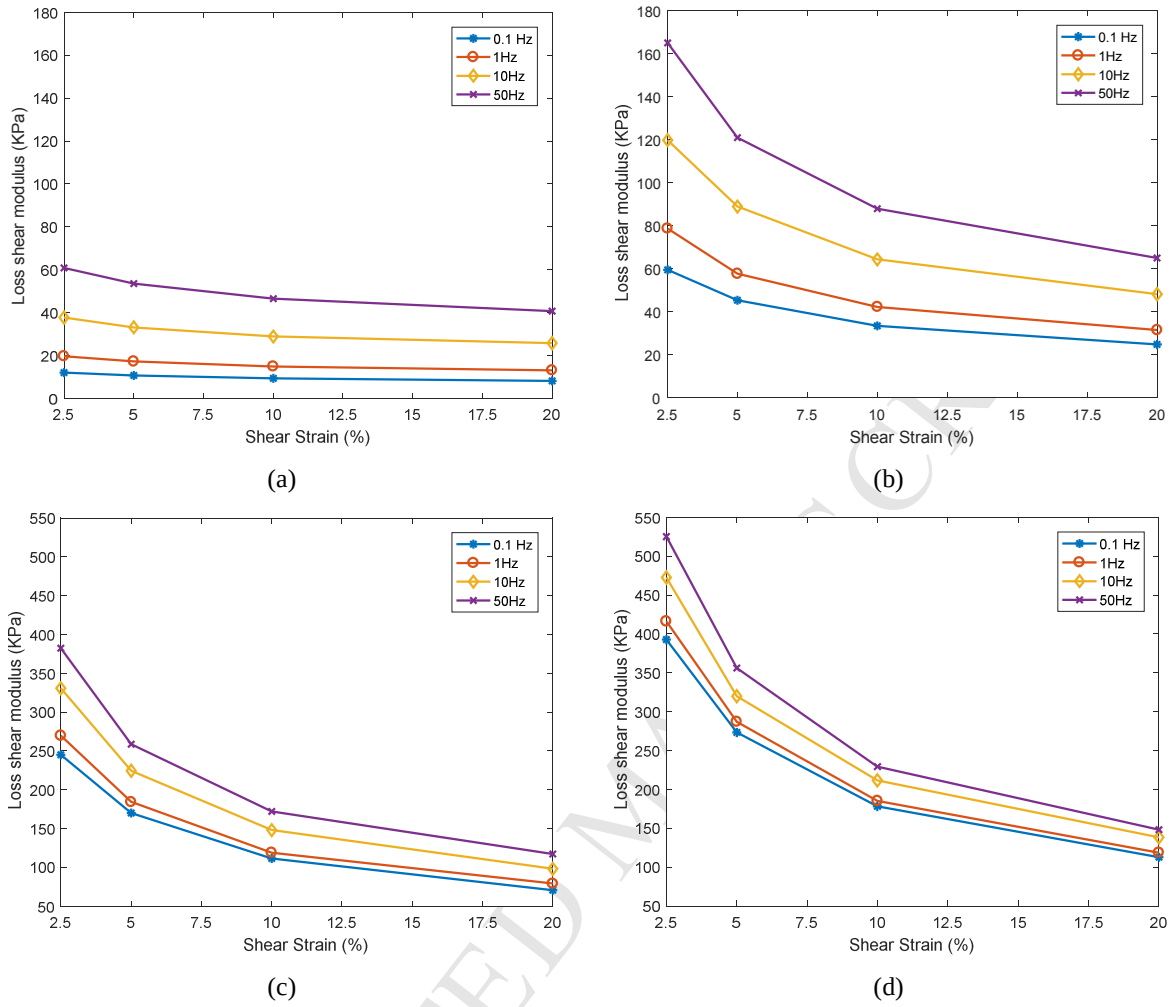

Figure 12: Effect of strain amplitude on the loss shear modulus of the MRE at different excitation frequencies and levels of magnetic flux density: (a) 0mT; (b) 150mT; (c) 300mT; and (d) 450mT.

4.2.3 Effect of magnetic flux density

Figure 13 illustrates the effect of magnetic flux density on the measured stress-strain characteristics of the MRE subject to different amplitudes of shear deformation at a frequency of 10 Hz. The results show substantial increase in the slope and area bounded by the stress-strain hysteresis loops with increase in the applied magnetic flux density. These suggest substantial variations in the dynamic characteristics (stiffness and damping) of the MRE with varying magnetic field, as reported in many studies [6, 7]. These have invariably emphasized the potential performance benefits of the MREs, owing to the strong dependence of their dynamic behavior on the controllable magnetic flux, which is perhaps better characterized in terms of the shear moduli. The effects of varying the magnetic flux density on the resulting elastic and loss shear moduli of the MRE (*type 6*) are shown in Figs 14 and 15, respectively, for the ranges of strain amplitude and excitation frequency considered.

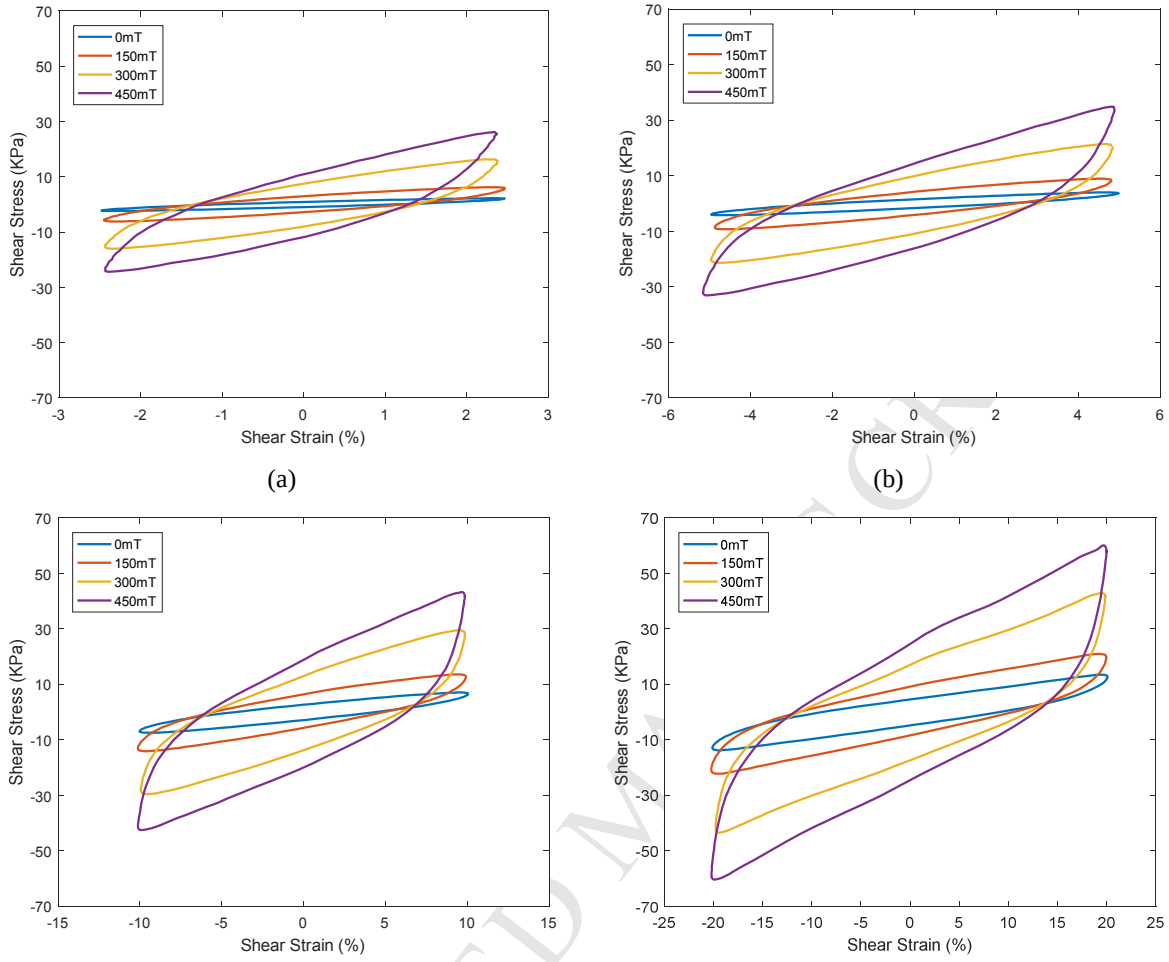

Figure 13: Effect of magnetic flux density on the measured stress-strain hysteresis loops of the MRE as a function of different strain amplitude at 10 Hz: (a) 2.5%; (b) 5%; (c) 10%; and (d) 20%.

The results show that both the elastic and loss shear moduli of the MRE increase substantially with increase in the magnetic flux, irrespective of the excitation frequency and the strain amplitude. The saturation in the elastic modulus is observed under higher flux density and 20% strain, as seen in Fig. 13(d). The saturation tendency in the loss modulus is notable under higher flux density for all strain amplitudes considered. The magnitudes of absolute and relative increases in the elastic and loss shear moduli of the MRE are substantially higher under lower strain amplitudes as well as lower excitation frequencies. For instance, increasing the magnetic flux density from 0 mT to 450 mT at the excitation frequency of 1 Hz causes the elastic shear modulus to increase from about 60kPa to nearly 893kPa (1383% relative increase) under 2.5 % shear strain. The corresponding relative increase in the elastic shear modulus under 20 % shear strain is only 422% (from nearly 51 kPa to 265 kPa) (422.72% relative increase). Table 5 summarizes the relative MR effect achieved under the application of 450 mT magnetic flux density under different loading conditions (strain amplitude and frequency). Up to 1672% increase in the MRE storage modulus is observed under 2.5% strain amplitude at the low frequency of 0.1, which decreases to about 252% under 20% strain amplitude

at 50 Hz. Such a substantial change in the relative MR effect of the MRE with relatively higher CIP fraction suggests its greater potential for applications in controllable vibration absorbers and isolators.

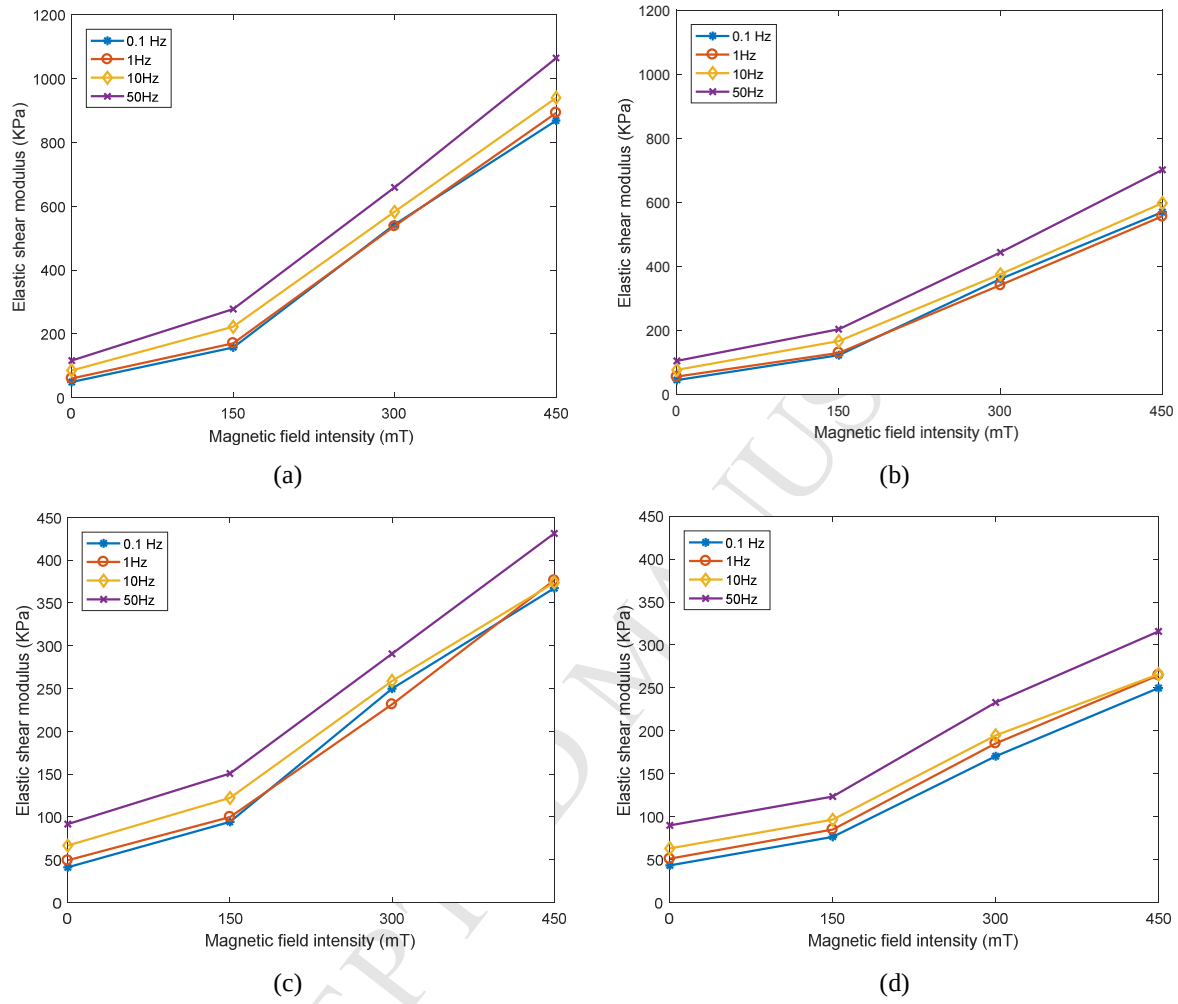

Figure 14: Effects of magnetic flux density on the elastic shear modulus of the MRE subject to different strain amplitudes at different excitation frequencies: (a) 2.5%; (b) 5%; (c) 10%; and (d) 20%.

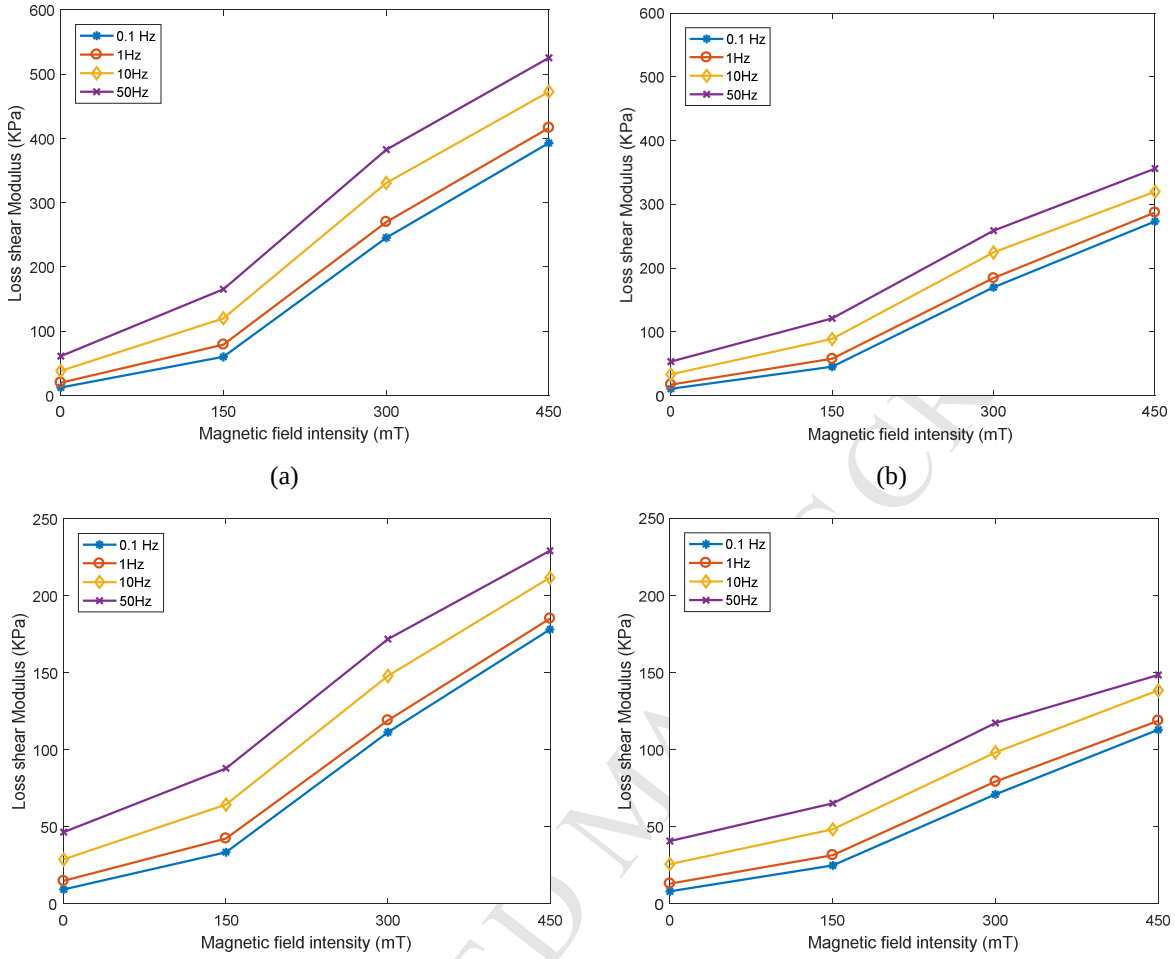

Figure 15: Effects of magnetic flux density on the loss shear modulus of the MRE subject to different strain amplitudes at different excitation frequencies: (a) 2.5%; (b) 5%; (c) 10%; and (d) 20%.

Table 5. Relative MR effect of the MRE (*type 6*) corresponding to 450 mT magnetic flux density and different loading conditions.

Strain amplitude (%)	Frequency (Hz)	Relative MR effect (0 mT to 450 mT)	Strain amplitude (%)	Frequency (Hz)	Relative MR effect (0 mT to 450 mT)
2.5	**0.1**	1672.1%	**10**	**0.1**	796.48%
2.5	**1**	1383.66%	**10**	**1**	666.21%
2.5	**10**	1002.28%	**10**	**10**	464.01%
2.5	**50**	815.44%	**10**	**50**	371.32%
5	**0.1**	1193.77%	**20**	**0.1**	510.21%
5	**1**	924.46%	**20**	**1**	422.72%
5	**10**	691.64%	**20**	**10**	323.83%
5	**50**	574.73%	**20**	**50**	252.66%

5. Conclusions

This study presents static and dynamic characteristics of MREs, fabricated in the laboratory, using the methods defined in ISO-1827 and ISO-4664 under broader ranges of excitation frequency and strain amplitude. Apart from the significant effect of the ferromagnetic particle content, the MRE with a softening agent revealed substantial gain in the relative MR effect. Increasing the iron particle content beyond the critical value can yield substantially higher MR effect provided that an adequate level of a softening agent is used. The dynamic properties of the MRE with 40% iron particle volume fraction revealed significant hysteresis in stress-strain data, which was symmetric in the simple shear mode. Both the slope and area bounded by the stress-strain hysteresis loop, which relate to elastic and loss shear moduli, showed strong and coupled dependence on the loading condition (strain amplitude and rate) and the applied magnetic flux density. The hysteresis loops showed nearly visco-elastic behavior of the MRE in the absence of the magnetic field but non-linear properties with increasing magnetic flux, strain amplitude and frequency. The nonlinear behavior was attributed to strain softening, strain-rate stiffening, and magnetic field stiffening or saturation phenomena. With the application of a 450 mT magnetic flux, the MRE revealed up to 1672% increase in the storage shear modulus under 2.5% strain amplitude at a frequency of 0.1, which decreased to nearly 252% under 20% strain amplitude at a frequency of 50 Hz. The potential for realizing such a substantial gain in the MR effect suggests highly promising features of the MRE with higher iron particle fraction for applications in adaptive noise and vibration control.

Acknowledgement

Financial support from Natural Sciences and Engineering Research Council of Canada (NSERC) is gratefully acknowledged.

References

[1] J. M. Ginder, M. E. Nichols, L. D. Elie, and S. M. Clark, "Controllable-stiffness components based on magnetorheological elastomers", Proceedings-SPIE The international Society for Optical Engineering, 2000;3985:418-425.

[2] S. Sun, H. Deng, J. Yang, W. Li, H. Du, G. Alici, and M. Nakano, “An adaptive tuned vibration absorber based on multilayered MR elastomers”, Smart Materials and Structures, 2015;24(4):045045.

[3] Z. Yang, C. Qin, Z. Rao, N. Ta, and X. Gong, “Design and analyses of axial semi-active dynamic vibration absorbers based on magnetorheological elastomers”, Journal of Intelligent Material Systems and Structures, 2014;25(17):2199-2207.

[4] H.X. Deng, X.l. Gong, and L.H. Wang, “Development of an adaptive tuned vibration absorber with magnetorheological elastomer”, Smart Materials and Structures, 2006;15(5):N111.

[5] S. Sun, Y. Chen, J. Yang, T. Tian, H. Deng, W. Li, H. Du, and G. Alici, “The development of an adaptive tuned magnetorheological elastomer absorber working in squeeze mode”, Smart Materials and Structures, 2014;23(7):075009.

[6] M. Behrooz, X. Wang, and F. Gordaninejad, “Modeling of a new semi-active/passive magnetorheological elastomer isolator”, Smart Materials and Structures, 2014;23(4):045013.

[7] J. Yang, H. Du, W. Li, Y. Li, J. Li, S. Sun, and H. Deng, “Experimental study and modeling of a novel magnetorheological elastomer isolator”, Smart Materials and Structures, 2013;22(11):117001.

[8] Y. Li, J. Li, T. Tian, and W. Li, “A highly adjustable magnetorheological elastomer base isolator for applications of real-time adaptive control”, Smart Materials and Structures, 2013;22(9):095020.

[9] H. Du, W. Li, and N. Zhang, “Semi-active variable stiffness vibration control of vehicle seat suspension using an MR elastomer isolator”, Smart Materials and Structures, 2011;20(10):105003.

[10] S. Sun, J. Yang, H. Deng, H. Du, W. Li, G. Alici, and M. Nakano, “Horizontal vibration reduction of a seat suspension using negative changing stiffness magnetorheological elastomer isolators”, International Journal of Vehicle Design, 2015;68:104-118.

[11] B. Kavlicoglu, B. Wallis, H. Sahin, and Y. Liu, 2011, "Magnetorheological elastomer mount for shock and vibration isolation", Active and passive smart structures and integrated systems, International Society for Optics and Photonics, vol. 7977, pp. 79770Y.

[12] S. Aguib, A. Nour, B. Benkoussas, I. Tawfiq, T. Djedid, and N. Chikh, “Numerical simulation of the nonlinear static behavior of composite sandwich beams with a magnetorheological elastomer core”, Composite Structures, 2016;139:111-119.

[13] W. Li, K. Kostidis, X. Zhang, and Y. Zhou, "Development of a force sensor working with MR ", Advanced Intelligent Mechatronics, IEEE/ASME International Conference, 2009:233-238.

[14] H. Böse, R. Rabindranath, and J. Ehrlich, “Soft magnetorheological elastomers as new actuators for valves”, Journal of Intelligent Material Systems and Structures, 2012;23(9):989-994.

[15] J. D. Carlson, and M. R. Jolly, “MR fluid, foam and elastomer devices”, Mechatronics, 2000;10(4–5):555-569.

[16] Jacobs, I.S. and Bean, C.P, “Fine Particles; Superparamagnetism,” Magnetism 3, Academic Press, New York, 1963;272.

[17] M. Mahdiani, F. Soofivand, F. Ansari, and M. Salavati-Niasari, “Grafting of CuFe12O19 nanoparticles on CNT and graphene: Eco-friendly synthesis, characterization and photocatalytic activity,” Journal of Cleaner Production, 2018;176:1185-1197.

[18] F. Ansari, A. Sobhani, and M. Salavati-Niasari, “Simple sol-gel synthesis and characterization of new CoTiO3/CoFe2O4 nanocomposite by using liquid glucose, maltose and starch as fuel, capping and reducing agents,” Journal of colloid and interface science, 2018;514:723-732.

[19] R. J. Mark, J. D. Carlson, and C. M. Beth, “A model of the behaviour of magnetorheological materials”, Smart Materials and Structures, 1996;5(5):607.

[20] M. Lokander, and B. Stenberg, “Performance of isotropic magnetorheological rubber materials”, Polymer Testing, 2003;22(3):245-251.

[21] L. Yancheng, L. Jianchun, L. Weihua, and D. Haiping, “A state-of-the-art review on magnetorheological elastomer devices”, Smart Materials and Structures, 2014;23(12):123001.

[22] V. Hossein, N. Mahmood, A. Seyed Masoud Sajjadi, and K. S. Stoyan, “A novel phenomenological model for dynamic behavior of magnetorheological elastomers in tension–compression mode”, Smart Materials and Structures, 2017;26(6):065011.

[23] M. Lokander, and B. Stenberg, “Improving the magnetorheological effect in isotropic magnetorheological rubber materials,” Polymer Testing, 2003;(6):677-680.

[24] T. Shiga, A. Okada, and T. Kurauchi, “Magnetroviscoelastic behavior of composite gels”, Journal of Applied Polymer Science, 1995;58(4):787-792.

[25] M. R. Jolly, J. D. Carlson, B. C. Muñoz, and T. A. Bullions, “The Magnetoviscoelastic Response of Elastomer Composites Consisting of Ferrous Particles Embedded in a Polymer Matrix”, Journal of Intelligent Material Systems and Structures, 1996;7(6):613-622.

[26] J. M. Ginder, M. E. Nichols, L. D. Elie, and J. L. Tardiff, "Magnetorheological elastomers: properties and applications", In Smart Structures and Materials, Smart Materials Technologies, 1999;3675:131-139.

[27] C. Bellan, and G. Bossis, “Field dependence of viscoelastic properties of MR elastomers”, International Journal of Modern Physics B, 2002;16(17-18):2447-2453.

[28] M. Farshad, and A. Benine, “Magnetoactive elastomer composites”, Polymer testing, 2004;23(3):347-353.

[29] M. Kallio, "The elastic and damping properties of magnetorheological elastomers", (Finland: VTT Publications), 2005:57.

[30] X. Gong, X. Zhang, and P. Zhang, “Fabrication and characterization of isotropic magnetorheological elastomers,” Polymer testing, 2005;24(5):669-676.

[31] P. R. von Lockette, J. Kadlowec, and J.-H. Koo, "Particle mixtures in magnetorheological elastomers (MREs)", In Smart Structures and Materials 2006: Active Materials: Behavior and Mechanics, 2006;6170:61700T.

[32] G. Stepanov, S. Abramchuk, D. Grishin, L. Nikitin, E. Y. Kramarenko, and A. Khokhlov, “Effect of a homogeneous magnetic field on the viscoelastic behavior of magnetic elastomers”, Polymer, 2007;48(2):488-495.

[33] A. A. Lerner, and K. A. Cunefare, “Performance of MRE-based vibration absorbers”, Journal of Intelligent Material Systems and Structures, 2008;19(5):551-63.

[34] H. Böse, and R. Röder, "Magnetorheological elastomers with high variability of their mechanical properties", InJournal of physics: Conference series 2009, IOP Publishing, 2009;149(1):012090.

[35] H.J. Jung, S.J. Lee, D.D. Jang, I.H. Kim, J.H. Koo, and F. Khan, “Dynamic characterization of magneto-rheological elastomers in shear mode”, IEEE transactions on magnetics, 2009;45(10):3930-3933.

[36] W. Li, Y. Zhou, and T. Tian, “Viscoelastic properties of MR elastomers under harmonic loading”, Rheologica acta, 2010;49(7):733-740.

[37] K. Danas, S. Kankanala, and N. Triantafyllidis, “Experiments and modeling of iron-particle-filled magnetorheological elastomers”, Journal of the Mechanics and Physics of Solids, 2012;60(1):120-138.

[38] F. Gordaninejad, X. Wang, and P. Mysore, “Behavior of thick magnetorheological elastomers”, Journal of Intelligent Material Systems and Structures, 2012;23(9):1033-1039.

[39] Y. Li, J. Li, W. Li, and B. Samali, “Development and characterization of a magnetorheological elastomer based adaptive seismic isolator”, Smart Materials and Structures, 2013;22(3):035005.

[40] I. Agirre-Olabide, J. Berasategui, M. J. Elejabarrieta, and M. M. Bou-Ali, “Characterization of the linear viscoelastic region of magnetorheological elastomers”, Journal of Intelligent Material Systems and Structures, 2014;25(16):2074-2081.

[41] S. Sun, H. Deng, J. Yang, W. Li, H. Du, and G. Alici, “Performance evaluation and comparison of magnetorheological elastomer absorbers working in shear and squeeze modes”, Journal of Intelligent Material Systems and Structures, 2015;26(14):1757-1763.

[42] Y. Yu, Y. Li, J. Li, and X. Gu, “A hysteresis model for dynamic behaviour of magnetorheological elastomer base isolator”, Smart Materials and Structures, 2016;25(5):055029.

[43] M. Norouzi, S. M. S. Alehashem, H. Vatandoost, Y. Q. Ni, and M. M. Shahmardan, “A new approach for modeling of magnetorheological elastomers”, Journal of Intelligent Material Systems and Structures, 2015;27(8):1121-35.

[44] K. M. Popp, M. Kröger, W. h. Li, X. Z. Zhang, and P. B. Kosasih, “MRE properties under shear and squeeze modes and applications”, Journal of Intelligent Material Systems and Structures, 2010;21(15):1471-1477.

[45] Y. Wan, Y. Xiong, and S. Zhang, “Temperature Dependent Dynamic Mechanical Properties of Magnetorheological Elastomers: Experiment and Modeling”, Composite Structures, 2018 (Accepted Manuscript).

[46] H. S. Jung, S. H. Kwon, H. J. Choi, J. H. Jung, and Y. G. Kim, “Magnetic carbonyl iron/natural rubber composite elastomer and its magnetorheology”, Composite Structures, 2016;136:106-112.

[47] A. Dargahi, “Fabrication, Characterization and Modeling of Magnetorheological Elastomers,” Masters Thesis, Concordia University, 2017; 98-102.

[48] ISO 1827, "Rubber, vulcanized or thermoplastic - Determination of shear modulus and adhesion to rigid plates - Quadruple-shear methods", International Standards Organization, Geneva, 2011.

[49] ISO 4664-1, "Rubber, vulcanized or thermoplastic - Determination of dynamic properties. Part 1: General guidance," International Standards Organization, Geneva, 2011.

[50] Y. Shen, M. F. Golnaraghi, and G. Heppler, “Experimental research and modeling of magnetorheological elastomers”, Journal of Intelligent Material Systems and Structures, 2004;15(1):27-35.

[51] L. Mullins, “Softening of rubber by deformation,” Rubber chemistry and technology, 1969;42(1),:339-362.

[52] D. Besdo, and J. Ihlemann, “Properties of rubberlike materials under large deformations explained by self-organizing linkage patterns”, International Journal of Plasticity, 2003;19(7):1001-1018.

[53] L. Chen, X. Gong, and W. Li, “Effect of carbon black on the mechanical performances of magnetorheological elastomers”, Polymer testing, 2008;27(3):340-345.

[54] J. S. Bergström, and M. C. Boyce, “Constitutive modeling of the large strain time-dependent behavior of elastomers”, Journal of the Mechanics and Physics of Solids, 1998;46(5):931-954.